



Derivation of Antarctic stratospheric sulfuric acid profiles and nucleation modeling of the polar stratospheric CN layer

Steffen Münch^{1,*}, Joachim Curtius¹

¹Institute for Atmospheric and Environmental Sciences, Goethe University Frankfurt am Main, Frankfurt am Main, 60323, Germany

* now at: Institute for Atmospheric and Climate Science, ETH Zürich, Zürich, 8092, Switzerland

Correspondence to: Steffen Münch (steffen.muench@env.ethz.ch)

Abstract. Recent analysis of long-term balloon-borne measurements of Antarctic stratospheric condensation nuclei (CN) and temperature combined with global model calculations showed the wide extent of a mid stratospheric layer of new particles. Here the nucleation model SAWNUC is used to derive Antarctic stratospheric gaseous sulfuric acid profiles and to investigate the nucleation process of this CN layer. The sulfuric acid profiles were derived for an altitude range of 18-32 km between July and October by simulating air parcel trajectories that descend inside the polar vortex and calculating the sulfuric acid amount that reproduces the observations. The derived sulfuric acid concentrations (volume mixing ratios) are of the order of magnitude of 10^4 cm^{-3} (10^{-14}) in July. In the following months the concentrations increase to about 10^7 cm^{-3} (10^{-11}) in October. They depend strongly on the temperature because a given temperature leaves only a small sulfuric acid range to reproduce the observed magnitude of CN. Ion-induced nucleation occurs. However, while it dominates nucleation at higher temperatures it has no significant influence on the nucleation rates at lower temperatures. Preexisting particles significantly reduce nucleation at sulfuric acid mixing ratios below 1 ppt. First estimates of sulfuric acid production rates range from 0.5 to about 500 molecules $\text{cm}^{-3} \text{ s}^{-1}$. A production mechanism for gaseous sulfuric acid during the Antarctic winter seems to be necessary to fully explain the observations. The derived sulfuric acid profiles compare well with mid-latitude and Arctic sulfuric acid concentrations.

1 Introduction

When investigating the condensation nuclei layer in the stratosphere, condensation nuclei (CN) are defined as all aerosol particles that are large enough to be measured by a CN-counter but too small to be measured by an optical particle counter, typically covering a range of particle diameters between ~ 10 and 300 nm. The particles in the CN layer are assumed to be formed by ion-induced or neutral homogeneous nucleation of sulfuric acid and water (binary nucleation).

Rosen and Hofmann (1983) first observed an increase of volatile CN at 25-30 km altitudes during winter at Laramie, Wyoming (41°N). They assumed the CN to be freshly nucleated sulfuric acid water particles with the polar stratosphere as the source region. Above McMurdo Station, Antarctica (78°S), Hofmann and Rosen (1985) also observed an increased CN concentration between 20 and 25 km after sunrise (CN layer). To check if the occurrence of this CN layer was an annual



polar phenomenon further measurements were performed which also observed the formation of a CN layer after sunrise (e.g. Hofmann (1990) at Kiruna, Sweden (68°N)). Therefore, sulfuric acid production by sunlight after the end of the polar night was suggested as the nucleation source.

With these observations modeling started to investigate the formation of the CN layer. Nucleation rate calculations by Hamill et al. (1990) indicated that binary nucleation could occur in the polar winter stratosphere if sulfuric acid concentrations were high enough. Zhao et al. (1995) developed a one-dimensional (altitude) aerosol model that showed that the transformation of OCS to SO₂ and further oxidation of SO₂ to H₂SO₄ are too slow to reproduce the observed CN increase. However, they could reproduce the formation of the CN layer when they added downward transport of SO₂ from the mesosphere inside the polar vortex. Mills et al. (1999) and Mills et al. (2005) presented modeling with a two dimensional (altitude and latitude) aerosol model that was able to reproduce the formation of the CN layer when including production of mesospheric SO₂ by photolysis of sulfuric acid and SO₃ (see also Vaida et al., 2003).

In summary, SO₂ is produced in the mesosphere by H₂SO₄ photolysis. During polar winter, more SO₂ is transported downward inside the polar vortex without being oxidized by photochemical reactions. After sunrise, this SO₂ is oxidized to sulfuric acid which initiates nucleation in the cold polar stratosphere and forms the CN layer.

15

More recently, Campbell and Deshler (2014) presented averaged balloon-borne CN measurements between 15 and 35 km above McMurdo Station, Antarctica (78°S) that were performed continuously for 24 years. They capture the already existing CN with concentrations around 20 cm⁻³ in June/July as well as the layer's development at 20-25 km to concentrations of up to 100 cm⁻³ from August until October during sunrise and warming by presenting monthly averaged CN concentration and temperature profiles.

20

Campbell et al. (2014) used a 3-dimensional chemistry climate model (Hurrell et al., 2013, English et al., 2011) and revealed the global extent of the CN layer. They simulated the year 2010 and compared the results to measurements above McMurdo Station (Campbell et al., 2014). The model reproduces the CN layer but at higher altitudes (around 30 km in the model vs. around 23 km in the observations). As an explanation they suggested (among others) biases in the critical nucleation variables: temperature, sulfuric acid and water concentration. However, there are no Antarctic stratospheric sulfuric acid measurements. Therefore, they inverted the nucleation equation to calculate the sulfuric acid concentration that corresponds to the CN increase over three weeks between two measurements. Their derived profile indicates that in the global model the sulfuric acid also has a shift towards higher altitudes which could explain the altitude shift of the simulated CN layer.

25

The approach of deriving a sulfuric acid profile from the measured CN is intriguing. However, they did invert a nucleation formulation that describes the nucleation with only one equation. No ion-induced nucleation, coagulation, or losses to preexisting particles were considered during the inversion. Therefore in this study, we use the nucleation model SAWNUC, which simulates all these processes, to derive the Antarctic stratospheric sulfuric acid profiles and to investigate the

30



processes that influence the nucleation of the CN layer. We also derived estimates of the corresponding sulfuric acid production rates.

The model and the derivation process are described in Sect. 2. The derived profiles, the role of ion-induced nucleation, the uncertainties and estimated sulfuric acid production rates are presented and discussed in Sect. 3. Then, the derived profiles are compared to the global modeling of Campbell et al. (2014) in Sect. 4.

2 Methods

2.1 The SAWNUC model

The SAWNUC model (Sulfuric Acid Water NUceation model, Lovejoy et al., 2004) simulates binary sulfuric acid water neutral and ion-induced nucleation. It explicitly simulates the step-by-step addition of sulfuric acid molecules in linear size bins for cluster sizes below 2 nm. Above 2 nm the particle concentrations are collected in geometric size bins. Here, 30 size bins with a geometric scale factor of 1.7 were used which range up to about 400 nm. Neutral and negatively charged clusters were simulated. For each size bin, SAWNUC simulates condensation and evaporation of sulfuric acid, coagulation with neutral clusters, recombination of negative clusters with positive ions, and losses to preexisting particles or chamber walls. Condensation, coagulation, and preexisting loss rates are calculated based on the hard sphere collision theory of Fuchs (1964). For the charged clusters, the Coulomb forces are calculated based on the intercluster potentials (Yu and Turco, 1998). For the neutral clusters, thermodynamic stabilities were calculated with the On-line Aerosol Inorganics Model (Carslaw et al., 1995). The neutral thermodynamics are adjusted to reproduce experimental nucleation rates of Ball et al. (1999). The thermodynamic stabilities of the negative clusters are calculated with the Thomson equation. However for small clusters, the values reported by Froyd and Lovejoy (2003a) and Lovejoy and Curtius (2001) are directly implemented into the model, which are based on experimental values and quantum chemical calculations (for more details see Lovejoy et al., 2004). For the neutral dimer and trimer, the thermodynamic stabilities presented by Hanson and Lovejoy (2006) are also implemented into the model. The SAWNUC model (Lovejoy et al., 2004) has been previously used (among others) in Ehrhart and Curtius (2013) and its parameterized version PARNUC (Kazil and Lovejoy, 2007) in Kirkby et al. (2011).

For this study the SAWNUC model was extended. Coagulation rates between neutral clusters are now calculated including van der Waals forces according to Chan and Mozurkewich (2001). The updated sulfuric acid dimer stabilities reported by Kürten et al. (2015) can be used for the simulation. The model code was redesigned to allow ambient condition changes during a simulation. Also the ability to perform multiple simulations within one program run was added and is used for the model “inversion“ in this study.

2.2 Deriving the profiles

This section describes the derivation of the Antarctic stratospheric sulfuric acid profiles. The profiles are based on the measured CN concentrations and temperatures above McMurdo Station, Antarctica (78°S) as presented by Campbell and



Deshler (2014, Fig. 1). Corresponding sulfuric acid concentrations and mixing ratios were derived for the time interval of June/July to October at altitudes from 18 km to 32 km. The SAWNUC model was “inverted“ by performing multiple simulations with the same ambient conditions but varying sulfuric acid concentrations, and searching for the sulfuric acid concentration that reproduces the observed CN. Thereby, all effects like coagulation, ions and preexisting particles are included in the inversion process.

2.2.1 Ambient parameters

To perform a simulation with SAWNUC, values for the following ambient parameters are needed: pressure, temperature, relative humidity, sulfuric acid concentration, ion pair production rate, as well as surface area and diameter of preexisting particles. CN concentrations and sizes for every time step are the model output. As the model was inverted, CN concentrations were also needed to search for the sulfuric acid concentrations.

Temperatures and CN concentrations were taken from Fig. 1 (Campbell and Deshler, 2014). The CN concentrations were compared with the measurements by summing over all CN concentrations with sizes above a detection limit (5 nm diameter was used in this study). Altitudes were converted to pressures according to the global modeling of Campbell et al. (2014).

The ionization rate of the Antarctic stratosphere in August-September 2010 was $3e5$ ion pairs per gram of air and second (Ilya Usoskin, personal communication, 2013; according to Usoskin et al., 2011).

The water vapor profile was chosen to be a linear increase from 3.0 to 6.0 ppm from 18 km to 25 km and then a constant value of 6.0 ppm up to 32 km in July. This profile was moved down by 1 km every month (to represent diabatic descent within the polar vortex).

The diameter of preexisting particles was assumed to be 100 nm. A surface area of $0.2 \mu\text{m}^2 \text{cm}^{-3}$ was chosen for 215.15 K and 30 km altitude, which is consistent with Zhao et al. (1995) who reported that the subsiding mesospheric air is very clean and with Campbell et al. (2014) reporting a surface area of $0.3 \mu\text{m}^2 \text{cm}^{-3}$ for 20-30 km altitude in early August 2010. This surface area was converted to each temperature/height combination according to the ideal gas equation.

Sensitivity tests concerning the influence of all these input values on the derived profiles were performed and are presented in Sect. 3.2.

2.2.2 The CN layer trajectory

With the described model setup, the sulfuric acid profiles were derived by using the SAWNUC model as a box model, simulating the nucleation process inside air parcels over the period of the four months. The most important air parcel trajectory for this study is the one that connects the monthly maximum of the measured CN (in the following termed “maximum trajectory”). It is assumed that this maximum of the particle concentration resides in a single air parcel that descends inside the polar vortex. This section describes the derivation process of the sulfuric acid values in the maximum trajectory.



Sulfuric acid concentrations were searched for on a monthly basis as the measured input values (CN and temperature) are also monthly averages. The ambient conditions and the sulfuric acid concentration were set at the beginning of a month and kept constant for the entire month. Simulation results were evaluated for each month. The simulated CN concentrations averaged over the month were compared to the measured values. If there were too many, the input sulfuric acid concentration was decreased and the model run was repeated. If the model did not produce enough CN, the input sulfuric acid concentration was increased. This process was reiterated until the sulfuric acid concentration was determined that corresponds best to the measured monthly CN concentrations. This resulted in a derived sulfuric acid concentration of the simulated month.

This scheme was used for every month. The time evolution of temperature (representative for all ambient conditions), the derived sulfuric acid volume mixing ratios (converted from the concentrations), and the simulated CN concentrations (> 5 nm) of the maximum trajectory's boxmodel simulation are shown in Fig. 1a. The derivation process is divided into five periods: the initialization phase and the June/July, August, September, and October periods (June/July are combined as the measurements in Campbell and Deshler, 2014, also combine these months).

Model initialization is necessary as some CN should already be present at the beginning of the first derived month. However, as the CN concentrations before June are not known, the trajectory simulation was started with an initialization phase from May 1st to June 15th, in which it builds up 110% of the June/July CN amount at June/July ambient conditions. This extra 10% was chosen because CN concentrations are expected to be higher at the beginning of the June/July period than at its end (because of missing sulfuric acid production and air compression, see below).

The June/July sulfuric acid concentration was derived by searching for the sulfuric acid concentration that reproduces the measured June/July CN amount. This sulfuric acid concentration is lower than during the initialization period as no new particles have to form and the existing ones have to decrease in number.

At the beginning of August the ambient conditions were changed to the August conditions (see temperature change in Fig. 1a). As the pressure increases during the descent of the air, this ambient change also includes a compression of the air volume and thereby an increase in the CN per cm^3 . This is seen in the CN jump at the beginning of August. The compression due to pressure increase is stronger than the expansion due to the temperature increase (both were calculated and combined). After the air compression, the sulfuric acid concentration was searched that reproduces the measured August mean CN amount. Here, a decrease from the compression-increased CN amount is necessary. Therefore, what seems like an increase in CN from July to August in the maximum trajectory values turns out to be a decrease due to the adiabatic compression.

At September 1st the ambient conditions were changed to the September conditions, the CN were compressed (only a small change can be discerned in Fig. 1a), and the sulfuric acid concentration was searched for that reproduces the September CN amount.

Finally in October the same procedure was used. Unfortunately, the use of a month-long time interval for temperature and sulfuric acid concentration produces an undesired increase of CN at the beginning of October (additional to the volume compression). Stable clusters below the counting threshold of 5 nm still exist from September and rapidly grow due to the



strongly increased sulfuric acid concentration in October. Only later in the month, the CN amount decreases as only few new particles are produced while the old CN coagulate and are lost to preexisting particles. This unrealistic behavior can only be addressed by modeling at higher time resolution where the ambient conditions are changed more gently in shorter time steps.

5 Therefore, to avoid this undesired increase at the beginning of October and to reduce the „compression jumps“, the same derivation process was performed with shorter time steps of 5 days. However, time developments of altitude, temperature, and CN at the shorter time steps had to be assumed as the measured values are presented as monthly averages. The time developments were described by assumed functions for which the monthly mean values match with the measured values. Therefore, the simulated maximum trajectory with 5-day time steps (Fig. 1b) follows these assumed functions. The
10 adjustments of the CN concentration to the air compressions are still visible at the beginning of every time step, but they are much smaller compared to the monthly simulations as the ambient changes are much smaller. Comparing the monthly average of the 5-day sulfuric acid mixing ratios with the derived monthly values shows that the monthly simulation overestimates the derived sulfuric acid for June/July to September and underestimates it for October. However, the difference always stays below a factor of 2. As the derived mixing ratios in this study span over several orders of magnitude,
15 this is considered a reasonable agreement. This comparison strengthens the confidence in the monthly derived sulfuric acid values which are used in the rest of this study.

The derived values comprise four sulfuric acid concentrations / mixing ratios for the months June/July to October. Sulfuric acid is at very low mixing ratios (below 0.1 ppt) in July due to lack of sunlight and therefore absence of sulfuric acid
20 production during Antarctic winter. When sunlight returns in August, in the beginning the mixing ratio decreases further, as the gas phase sulfuric acid production takes some time to become larger than the losses (the chemical lifetime of SO₂ by OH and thereby the sulfuric acid production time is about a month at 20-30 km altitude; SPARC Report No.4 chapter 2.4.1). Starting in September, the sulfuric acid amount increases first slowly and then strongly from September to October by one order of magnitude reaching a maximum of ~1 ppt.

25 2.2.3 Complementing the profiles with more trajectories

To complement the profiles, more sulfuric acid mixing ratios were derived by simulating more trajectories that start at different altitudes. The trajectories are derived from the maximum trajectory by considering that the subsidence velocity decreases with decreasing altitude and that the polar vortex declines towards spring. Thereby, 23 trajectories starting at altitudes between 18 km and 40 km were simulated for this study. If the altitude was above 32 km, the initialization phase
30 was extended until the trajectory arrived below 32 km.

For all of these trajectories the procedure of deriving the corresponding sulfuric acid concentration was used as described above with two exceptions: First, at some points the temperature was a bit below 190 K (max. 4 K below) which is below SAWNUC's temperature range. Therefore these temperatures were fixed at 190 K. This introduces little uncertainty to these



values as the amount can be estimated with the sensitivity test concerning inter-annual temperature variations, presented below in Fig. 5d. Second, due to the design of the derivation process, the model was not able to reproduce the September CN amount of three trajectories in September at 27-28.5 km altitude. Therefore, the procedure was adjusted for these 3 data points, so that it does not search for the mean CN during this month but the CN are only required to match at the end of the month. This is also expected to introduce only a small additional uncertainty to these three September values as the specific CN amount only has a small influence on the derived sulfuric acid amount (see below).

Deriving the sulfuric acid concentrations and mixing ratios for all trajectories resulted in values for nearly every combination of month and altitude. All these values then were combined to the four derived Antarctic sulfuric acid profiles.

3 Results and discussion

The derived Antarctic sulfuric acid profiles are shown in Fig. 2. The general shape of the derived sulfuric acid profiles is plausible. In Antarctic winter the values are well below one part per trillion because there is no sulfuric acid production when the sunlight is missing. Then, with the return of sunlight in August the values increase at high altitudes and in September at all altitudes. In October, they reach maximum values of above 10 ppt. The reason for the higher sulfuric acid mixing ratios at high altitudes is probably that fairly large amounts of source SO₂ are transported downward from the mesosphere and that the actinic flux is high at these altitudes.

The figure also reveals that the temperature is the most important controlling variable for the sulfuric acid as the shapes of both profiles are very similar. This is because temperature and sulfuric acid concentration mainly determine the nucleation rate. A change in the sulfuric acid concentration by one order of magnitude leads to a change in the nucleation rate by also order(s) of magnitude. At a given temperature, there is a small sulfuric acid window where particle concentrations of 10 to 100 cm⁻³ magnitude can exist. The nucleation rate has to be in this small window, otherwise there would be by far too many, or, too few CN. This small window is determined by the temperature. Therefore, whether 20 or 50 particles are present has only little influence on the derived sulfuric acid as this only changes the sulfuric acid inside this small window. So from the two main input parameters of the derivation process, the temperature controls the derived sulfuric acid's order of magnitude and the exact CN amount decides about the decimal places. This is why the derived profiles look very similar to the temperature profiles and the CN layer's influence cannot be seen that clearly, however it is present indirectly as the magnitude of the CN defines the sulfuric acid window.

The derived sulfuric acid mixing ratios for October at altitudes above 25 km are very high. In fact the model calculations yield a particle distribution with a total sulfur mass that is higher than the total stratospheric sulfur at these altitudes. A detailed analysis reveals that at these high sulfuric acid mixing ratios the particles grow above 300 nm. However, as the measurements only counted particles below 300 nm, here the derivation mechanism fails. The reason for this is that at these high temperatures a water vapor mixing ratio of about 5 ppm leads to very low relative humidities and therefore very high particle evaporation rates. To compensate these high evaporation rates the derivation mechanism predicts these very high



sulfuric acid concentrations to reproduce the observed particle amount. Based on this analysis we conclude that it seems unlikely that the particles above 25 km in October (and maybe also at the highest altitudes in September) are volatile, pure sulfuric acid water particles as evaporation rates are too high. The measurements of Campbell and Deshler (2014) show that there are some non-volatile particles present especially at high altitudes towards spring and also Curtius et al. (2005) observed non-volatile particles in the Arctic lower stratosphere. Therefore, we assume that most of the October particles above 25 km are non-volatile and therefore cannot be simulated with the SAWNUC model. Nevertheless, we show the too high sulfuric acid values in Fig. 2 as dotted line for completeness but omit these values for the rest of the study.

The derived sulfuric acid profiles cannot be compared directly to data from in situ or remote sensing measurements of Antarctic stratospheric sulfuric acid as such data does not exist to our knowledge. However, northern mid-latitude balloon-borne measurements have been published (Arnold et al., 1981; Reiner and Arnold, 1997; Schlager and Arnold, 1987; Viggiano and Arnold, 1981). Mills et al. (2005) presented a summary of these measurements. A comparison of these measurements with our derived sulfuric acid concentrations shows good agreement (Fig. 3). The concentrations range from 10^4 cm^{-3} to above 10^7 cm^{-3} and they have a similar shape: low values at low altitudes with an increase to high values at high altitudes. Due to the different locations (43°N vs. 78°S) the altitudes cannot be compared directly as the tropopause is expected to be at lower altitudes above Antarctica. Therefore, our derived profiles should be shifted upwards for comparison which improves the agreement. Note that also the adiabatic expansion has to be considered when shifting the profiles upwards. The derived October profile has an uncertainty towards lower values (see below) which also increases the agreement with the measurements. The derived lower concentrations in June/July at high altitudes compared to mid-latitudes are an expected result of the spare sunlight during polar night. However, the low June/July concentrations are of the same order of magnitude as inferred Arctic sulfuric acid concentrations presented by Krieger and Arnold (1994) (Fig. 3). In summary, our derived profiles are generally in agreement with stratospheric sulfuric acid measurements from other latitudes.

3.1 Ion-induced nucleation

To study the role of ion-induced nucleation during the formation of the CN layer, the sulfuric acid profiles were derived again, but without simulating ions. The comparison is shown in Fig. 4. In some areas the removal of ions has nearly no effect on the derived profiles, however, in other areas the sulfuric acid mixing ratios increase by almost an order of magnitude. The regions that are most affected are the ones with higher temperatures. At low temperatures the neutral clusters are stable enough so that including an ion to the cluster does not increase its stability against evaporation in an amount that would change the nucleation rate. Therefore, even if ions are present and ion-induced nucleation occurs, it is not more efficient than neutral nucleation. At higher temperatures on the other hand, the neutral clusters are not as stable any more and including an ion to the clusters stabilizes them and increases the nucleation rate significantly. Thus to create the same amount of CN when no ions are present, more sulfuric acid is required than if ions were present simultaneously. In conclusion, in the areas of lower temperatures (which includes the formation area of the CN layer) the ions do not significantly influence the nucleation rate. However, in the areas of higher temperatures the CN are almost exclusively produced by ion-induced nucleation.



3.2 Sensitivity studies

To estimate the uncertainties of the derived sulfuric acid profiles, sensitivity tests were performed. Besides the 1-month time step for the derivation periods (already discussed in Sect. 2.2.2), significant uncertainties are mainly introduced by three factors: a) the uncertainty of the CN measurement cutoff size, b) the uncertainty of the climatological preexisting particle surface area, and c) uncertainties of the thermochemical data, the condensation and coagulation rates used in the SAWNUC model. The Antarctic stratospheric sulfuric acid is also expected to vary from year to year (e.g. depending on the strength of the diabatic descent of mesospheric air masses within the polar vortex).

3.2.1 CN measurement cutoff size

The first sensitivity test investigates the influence of the CN measurement cutoff size on the derived profiles. Campbell and Deshler (2014) reported that their CN counters' efficiencies were at around 75% for particles with 3 nm radius (6 nm diameter). So the 50% cutoff size should be below 6 nm diameter at the ground. However, they also reported that the cutoff could increase to 20 nm diameter at conditions of 20 km altitude. This, unfortunately, is a source of uncertainty for the measured CN concentrations.

For the derived profiles it was assumed that the measured CN are > 5 nm in diameter. For this sensitivity test the profiles were derived assuming a cutoff of 10 nm diameter. A higher cutoff means that the particles have to grow larger before they are counted, thus the required sulfuric acid concentrations have to increase in the nucleation areas. In October during the decay of the CN layer, the mixing ratios have to decrease though, because even if no nucleation occurs there still are stable, growing particles left that are smaller than the cutoff size. Therefore, the derived sulfuric acid mixing ratios would be smaller to produce less new CN and to keep the growth rates small enough so that some of these CN stay below the cutoff size. The result of this sensitivity test is shown in Fig. 5a and the predictions are confirmed. The July to September mixing ratios are higher and in October inside the CN layer the mixing ratios are lower. Therefore, the 50% cutoff uncertainty of the CN measurements has an impact on the derived profiles, especially on the October profile.

3.2.2 Preexisting particles surface area

The second sensitivity test investigates the influence of the total surface area of the preexisting particles. For the derived profiles a surface area of $0.2 \mu\text{m}^2 \text{cm}^{-3}$ at 30 km and 215.15 K was chosen, according to Campbell et al. (2014) reporting $0.3 \mu\text{m}^2 \text{cm}^{-3}$ for 20-30 km altitude in early August 2010, and converted to the temperature/pressure conditions according to the ideal gas law. For this sensitivity test the surface area was increased to $0.5 \mu\text{m}^2 \text{cm}^{-3}$ at 30 km and 215.15 K. The results show a significant influence on derived sulfuric acid mixing ratios below 1 ppt (Fig. 5b). In this area, mixing ratios increase by about a factor of 2 as at these conditions the losses to preexisting particles are in competition with the nucleation (Ehrhart and Curtius, 2013). Therefore, if the chosen surface area of $0.2 \mu\text{m}^2 \text{cm}^{-3}$ is not representative for all years, the derived profiles will have to be shifted either to higher or lower values according to this sensitivity test.



3.2.3 Model uncertainties

The third sensitivity test investigates the influence of the model uncertainties on the derived profiles. First, the uncertainty of the measured stabilities of the negatively charged clusters was tested according to Lovejoy et al. (2004) by adding 0.5 kcal to all changes in Gibbs free energy of negatively charged clusters. Second, all coagulation and condensation rates were reduced
5 by 20%. And third, the updated neutral sulfuric acid dimer thermodynamic stabilities presented by Kürten et al. (2015) were used for the calculations. They suggest a higher relative humidity dependence of the equilibrium constant of uncharged clusters which leads to higher dimer evaporation rates at low relative humidities.

The result of this combined sensitivity test is shown in Fig. 5c. An examination of the individual influences (not shown here) leads to the following conclusions: The changes of the thermodynamic values for the charged clusters influence the derived
10 mixing ratios in the area where ion-induced nucleation occurs. The changes due to the varied coagulation coefficients introduce a little shift to all values. The updated dimer stabilities with relative humidity dependence have a significant influence on the derived sulfuric acid mixing ratios in the regions of low relative humidity (higher temperature), but only if neutral binary nucleation dominates there.

3.2.4 Inter-annual variations and other tests

15 The last test estimates how the derived profiles may vary from year to year as this study used measurements averaged over 30 years. To estimate the inter-annual variations, all measured CN concentrations were increased by 60% and all temperatures were increased by 5 K. Both changes should lead to higher sulfuric acid values which is confirmed by the results (Fig. 5d). As the sulfuric acid profiles are mainly controlled by the temperature, the increase is mainly due to the temperature increase. The inter-annual variations are significant but they do not change the order of magnitude of the
20 profiles.

Additional sensitivity studies (not shown here) showed that the exact amount of ions or water molecules has only a very small influence on the derived profiles most probably because there are enough ions present and bigger changes than the stratospheric water vapor uncertainty of a few parts per million would be necessary to significantly change the derived profiles. Similarly, the CN and temperature measurement uncertainties (besides the cutoff uncertainty) have only a very little
25 influence on the derived profiles as the temperature uncertainty is very low. Adding hourly temperature variations generated according to a Gaussian distribution with mean value of 0 K and a standard deviation of 2 K to the 5 day maximum trajectory simulation had only a small influence on the derived sulfuric acid amounts.

3.2.5 Summary and discussion

Uncertainties are introduced by the model design of monthly derivation periods as the monthly values are an overestimation
30 in June/July to September and an underestimation in October. However, the cutoff measurement uncertainty leads to higher sulfuric acid values in June/July to September and lower values in October, so these two uncertainties are partly



compensating each other. For the October profile however, the uncertainty towards lower mixing ratios introduced by the uncertainty of the CN counter cutoff is bigger. At low sulfuric acid mixing ratios (<1ppt), the derived profiles have an uncertainty due to preexisting particles. The model uncertainties introduce uncertainties to the profiles towards higher or lower values at the areas of ion-induced nucleation and towards higher values at low relative humidities when neutral nucleation dominates. The sulfuric acid profiles are expected to vary from year to year. The June/July profile has some additional uncertainties which are discussed in the next section.

Therefore, the October profile should have the highest uncertainty, followed by the June/July profile. The August and September profiles should be the most accurate, which is during the formation of the CN layer.

3.3 Sulfuric acid production (estimate)

To estimate altitude profiles of the sulfuric acid production rates the modeling process had to be extended. As described, the sulfuric acid profiles were derived by searching for a constant sulfuric acid concentration that produces the measured CN amount. The extended approach was to assume a constant sulfuric acid production rate instead of a constant sulfuric acid concentration, and to simulate the sulfuric acid molecule concentration. The production was simulated by continually adding molecules throughout the modelled time periods. This added amount describes the net production (H_2SO_4 production from SO_2 minus H_2SO_4 photolysis to SO_2 , and potential other production processes). It does not contain the sulfuric acid that evaporates from freshly forming CN as this is now explicitly simulated by the model. However, the preexisting particles are not assumed to evaporate in the model, therefore this production term could also represent any sulfuric acid that evaporates from preexisting particles.

With this approach, sulfuric acid production profiles were derived with monthly production rates (Fig. 6). Their shapes look much like the derived sulfuric acid profiles, which is expected. They also range over 3-4 orders of magnitude from 0.5 to about $500 \text{ cm}^{-3} \text{ s}^{-1}$.

The June/July production rates need further investigation. They indicate that some (small) sulfuric acid production should occur even though there is nearly no sunlight during winter. This sulfuric acid could be produced by processes that do not require sunlight. Krieger and Arnold (1994) presented Arctic negative ion composition measurements and inferred gaseous sulfuric acid concentrations. They found strong evidence for an OH production process that does not require sunlight as they also observed sulfuric acid production during Arctic winter. They proposed OH production via ambient ions as additional sulfuric acid source and calculated a sulfuric acid production rate by ions of approximately $0.2\text{-}0.9 \text{ cm}^{-3} \text{ s}^{-1}$. Compared to our derived June/July production rates, these are lower (max. by one order of magnitude). This difference could be due to different ambient conditions in the Arctic compared to the Antarctic stratosphere or the OH production by ions explains our derived production rates only partly. Our derived sulfuric acid concentrations for June/July could be too high as the production and therefore the nature of the CN measured in June/July are unknown (there are no measurements in Antarctic fall). They could be more stable if they were not produced only by binary nucleation (but e.g. with meteoritic dust). Or they could be the result of an Antarctic fall nucleation event that was predicted by the global modeling of Campbell et al. (2014).



Estimates of Antarctic sulfuric acid production profiles are presented in Fig. 6. They do indicate some sulfuric acid production during Antarctic winter. However, they should only be considered as first estimates as they are one additional step away from the measurements. Processes like preexisting particle evaporation, OH production from cosmic rays, and CN production by other processes could influence the derived production profiles.

5 4 Comparison with global modeling of Campbell et al. (2014)

Our derived sulfuric acid profiles can now be compared to the global modeling of Campbell et al. (2014) to discuss the origin of the CN layer's altitude shift in their model. For this, we compare our derived sulfuric acid profiles to the global model simulation presented by Campbell et al. (2014) in Fig. 2. We compare the values between early July and late October. Our sulfuric acid volume mixing ratios were derived for the altitude range of 18 km to 32 km. In the global model, we find
10 corresponding sulfuric acid values roughly between 25 km and 38 km. In this range the high altitude July value and the low altitude October value match. Also high sulfuric acid mixing ratios at high October altitudes are found in the global model.

However, the global model simulates much lower sulfuric acid concentrations in July at low altitudes. They are the result of missing sunlight and therefore no sulfuric acid production. As discussed above, SAWNUC seems to predict sulfuric acid production in this region. However, as discussed, this production could need an additional process like OH production by
15 ions that can produce sulfuric acid without sunlight. As this additional process is not simulated by the global model, it predicts lower sulfuric acid mixing ratios in July at low altitudes. Therefore, it could be possible that the global model's minimum sulfuric acid mixing ratio of about $1 \cdot 10^{-20}$ is a strong underestimation.

Nevertheless, the general orders of magnitude of our derived sulfuric acid profiles are mostly found in the global model output, though with a 7 km altitude shift to higher altitudes. Thus, the global model has an altitude shift in CN, temperature,
20 and sulfuric acid. This is further strengthened by comparing the modelled SO_2 with satellite observations by Höpfner et al. (2013) which suggests an even stronger altitude shift. Thus our results support the suggestion by Campbell et al. (2014) that the altitude shift in their modelled CN layer seems to be a result of altitude shifts in the controlling variables of the nucleation.

Note however, that this result could increase the confidence in the simulated global extent of the CN layer. If only the
25 temperature had an altitude shift and not the sulfuric acid, at each altitude there would be very different temperature / sulfuric acid combinations, resulting in different nucleation rates compared to the real stratosphere. However, as the sulfuric acid also has an altitude shift, the nucleation rates should be closer to reality and therefore also the simulation of the global extent of the CN layer.



5 Summary

Balloon-born measurements of stratospheric CN above McMurdo Station, Antarctica, reveal the presence of a CN layer of freshly formed particles at 21-27 km altitude in August to October. Campbell et al. (2014) showed the global extent of this CN layer with a global model that reproduced the production of the CN layer by binary sulfuric acid water nucleation.

5 However, in their model the CN layer was located at too high altitudes. Unfortunately, no Antarctic stratospheric sulfuric acid measurements exist for comparison. Therefore, Campbell et al. (2014) derived sulfuric acid concentrations from the measured CN and temperatures. However, they did not use a microscopic nucleation model that includes processes such as coagulation, ion-induced nucleation, and losses to preexisting particles. Therefore, the goal of the present study was to use the nucleation model SAWNUC as a box model to derive Antarctic stratospheric sulfuric acid profiles based on their
10 measurements and to investigate the nucleation process.

The sulfuric acid profiles were derived for the altitudes of 18 - 32 km by simulating air parcel trajectories that descend inside the polar vortex. For each trajectory, monthly sulfuric acid values were derived by searching for the sulfuric acid amount that reproduces the observed CN at the given ambient conditions. The derived sulfuric acid concentrations (volume mixing ratios) are of the order of 10^4 cm^{-3} (10^{-14}) in July. In the following months the concentrations increase to about 10^7 cm^{-3} (10^{-11}) in October. They depend strongly on the temperature because at a given temperature the nucleation rate varies with the sulfuric acid amount, leaving only a small sulfuric acid window to reproduce the observed magnitude of CN. The derived sulfuric acid profiles compare well with measured mid-latitude profiles and also with inferred Arctic sulfuric acid concentrations.

Ion-induced nucleation occurs, however, at low temperatures it has no significant influence on the nucleation rates as the
20 neutral clusters are already stable enough, so that an additional charge does not significantly increase their stabilities. However, at higher temperatures the neutral clusters are not as stable anymore and ion-induced nucleation becomes the dominant nucleation mechanism.

Uncertainties of the derived profiles are caused by uncertainties of the instrumental cutoff diameter of the CN counter used for the measurements, the uncertainties of the preexisting particles surface area, and model uncertainties. The October profile
25 has an uncertainty towards lower values mainly due to the uncertainty of the CN measurement cutoff. Sulfuric acid mixing ratios below 1 ppt depend significantly on preexisting particles surface area. The profiles are expected to vary from year to year.

Estimates of sulfuric acid production rates range from 0.5 to about $500 \text{ molecules cm}^{-3} \text{ s}^{-1}$. Sulfuric acid production during Antarctic winter seems to be necessary to explain the measurements. This would require a second production process that
30 does not require sunlight (e.g. OH production by ambient ions). However, the production rates should only be considered as first estimates as they could be influenced by a variety of processes that were not simulated with this model.



Finally, a comparison of the derived sulfuric acid profiles with the global modeling of Campbell et al. (2014) strengthens the assumption that the global model represents the processes in general but at too high altitudes as also the sulfuric acid seems to be simulated at too high altitudes.

Acknowledgements

- 5 We thank Edward R. Lovejoy, Karl D. Froyd, Jan Kazil, and Sebastian Ehrhart for providing the SAWNUC code and Andreas Engel for useful discussion.

References

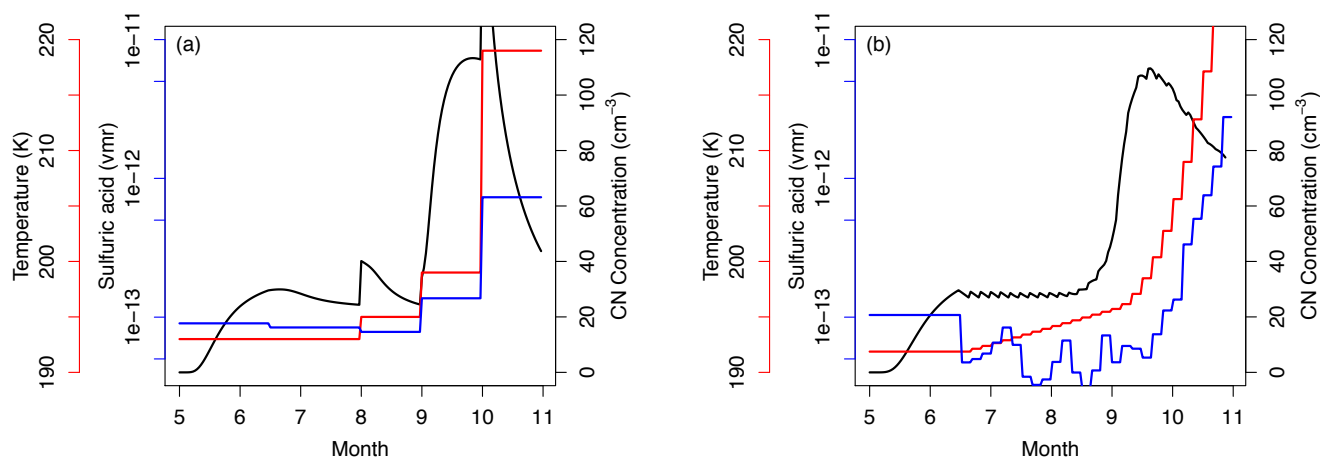
- Arnold, F., Fabian, R., and Joos, W. (1981). Measurements of the height variation of sulfuric acid vapor concentrations in the stratosphere. *Geophysical Research Letters*, 8(3), 293-296.
- 10 Ball, S. M., Hanson, D. R., Eisele, F. L., and McMurry, P. H. (1999). Laboratory studies of particle nucleation: Initial results for H₂SO₄, H₂O, and NH₃ vapors. *Journal of Geophysical Research: Atmospheres* (1984–2012), 104(D19), 23709-23718.
- Campbell, P., and Deshler, T. (2014). Condensation nuclei measurements in the midlatitude (1982–2012) and Antarctic (1986–2010) stratosphere between 20 and 35 km. *Journal of Geophysical Research: Atmospheres*, 119(1), 137-152.
- Campbell, P., Mills, M., and Deshler, T. (2014). The global extent of the mid stratospheric CN layer: A three-dimensional
15 modeling study. *Journal of Geophysical Research: Atmospheres*, 119(2), 1015-1030.
- Carslaw, K. S., Clegg, S. L., and Brimblecombe, P. (1995). A thermodynamic model of the system HCl-HNO₃-H₂SO₄-H₂O, including solubilities of HBr, from < 200 to 328 K. *The Journal of Physical Chemistry*, 99(29), 11557-11574.
- Chan, T. W., and Mozurkewich, M. (2001). Measurement of the coagulation rate constant for sulfuric acid particles as a function of particle size using tandem differential mobility analysis. *Journal of aerosol science*, 32(3), 321-339.
- 20 Curtius, J., Weigel, R., Vössing, H. J., Wernli, H., Werner, A., Volk, C. M., ... and Schlager, H. (2005). Observations of meteoric material and implications for aerosol nucleation in the winter Arctic lower stratosphere derived from in situ particle measurements. *Atmospheric chemistry and physics*, 5(11), 3053-3069.
- English, J. M., Toon, O. B., Mills, M. J., and Yu, F. (2011). Microphysical simulations of new particle formation in the upper troposphere and lower stratosphere. *Atmos. Chem. Phys.*, 11(17), 9303-9322.
- 25 Ehrhart, S., and Curtius, J. (2013). Influence of aerosol lifetime on the interpretation of nucleation experiments with respect to the first nucleation theorem. *Atmospheric Chemistry and Physics*, 13(22), 11465-11471.
- Froyd, K. D., and Lovejoy, E. R. (2003a). Experimental thermodynamics of cluster ions composed of H₂SO₄ and H₂O. 2. Measurements and ab initio structures of negative ions. *The Journal of Physical Chemistry A*, 107(46), 9812-9824.
- Froyd, K. D., and Lovejoy, E. R. (2003b). Experimental thermodynamics of cluster ions composed of H₂SO₄ and H₂O. 1.
30 Positive ions. *The Journal of Physical Chemistry A*, 107(46), 9800-9811.



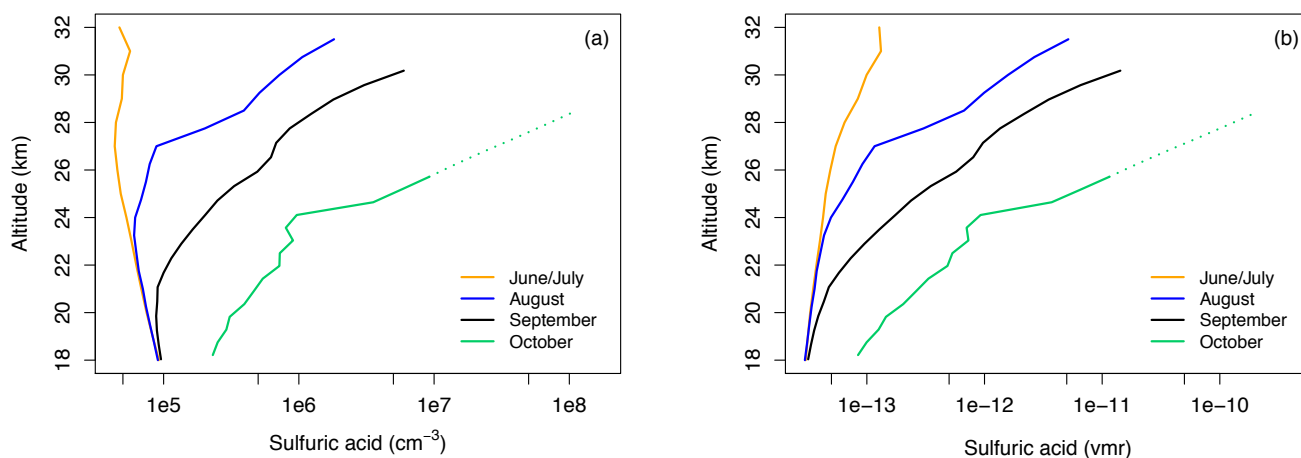
- Fuchs, N. A. (1964). The mechanisms of aerosols. Pergamon. New York.
- Hamill, P., Toon, O. B., and Turco, R. P. (1990). Aerosol nucleation in the winter Arctic and Antarctic stratospheres. *Geophysical Research Letters*, 17(4), 417-420.
- Hanson, D. R., and Lovejoy, E. R. (2006). Measurement of the thermodynamics of the hydrated dimer and trimer of sulfuric acid. *The Journal of Physical Chemistry A*, 110(31), 9525-9528.
- 5 Hofmann, D. J. (1990). Measurement of the condensation nuclei profile to 31 km in the Arctic in January 1989 and comparisons with Antarctic measurements. *Geophysical Research Letters*, 17(4), 357-360.
- Hofmann, D. J., and Rosen, J. M. (1985). Antarctic observations of stratospheric aerosol and high altitude condensation nuclei following the El Chichon eruption. *Geophysical Research Letters*, 12(1), 13-16.
- 10 Höpfner, M., Glatthor, N., Grabowski, U., Kellmann, S., Kiefer, M., Linden, A., ... and Boone, C. D. (2013). Sulfur dioxide (SO₂) as observed by MIPAS/Envisat: temporal development and spatial distribution at 15–45 km altitude. *Atmospheric Chemistry and Physics*, 13(20), 10405-10423.
- Hurrell, J. W., Holland, M. M., Gent, P. R., Ghan, S., Kay, J. E., Kushner, P. J., ... and Marshall, S. (2013). The community earth system model: A framework for collaborative research. *Bulletin of the American Meteorological Society*, 94(9), 1339-15 1360.
- Kazil, J., and Lovejoy, E. R. (2007). A semi-analytical method for calculating rates of new sulfate aerosol formation from the gas phase. *Atmospheric Chemistry and Physics*, 7(13), 3447-3459.
- Kirkby, J., Curtius, J., Almeida, J., Dunne, E., Duplissy, J., Ehrhart, S., ... and Stratmann, F. (2011). Role of sulphuric acid, ammonia and galactic cosmic rays in atmospheric aerosol nucleation. *Nature*, 476(7361), 429-433.
- 20 Krieger, A., and Arnold, F. (1994). First composition measurements of stratospheric negative ions and inferred gaseous sulfuric acid in the winter Arctic vortex: implications for aerosols and hydroxyl radical formation. *Geophysical research letters*, 21(13), 1259-1262.
- Kürten, A., Münch, S., Rondo, L., Bianchi, F., Duplissy, J., Jokinen, T., ... and Curtius, J. (2015). Thermodynamics of the formation of sulfuric acid dimers in the binary (H₂SO₄-H₂O) and ternary (H₂SO₄-H₂O-NH₃) system. *Atmospheric* 25 *Chemistry and Physics Discussions*, 15(10), 13957-14006.
- Lovejoy, E. R., Curtius, J., and Froyd, K. D. (2004). Atmospheric ion-induced nucleation of sulfuric acid and water. *Journal of Geophysical Research: Atmospheres* (1984–2012), 109(D8).
- Lovejoy, E. R., and Curtius, J. (2001). Cluster ion thermal decomposition (II): Master equation modeling in the low-pressure limit and fall-off regions. Bond energies for HSO₄-(H₂SO₄)_x (HNO₃)_y. *The Journal of Physical Chemistry A*, 105(48), 30 10874-10883.
- Mills, M. J., Toon, O. B., and Solomon, S. (1999). A 2D microphysical model of the polar stratospheric CN layer. *Geophysical research letters*, 26(8), 1133-1136.



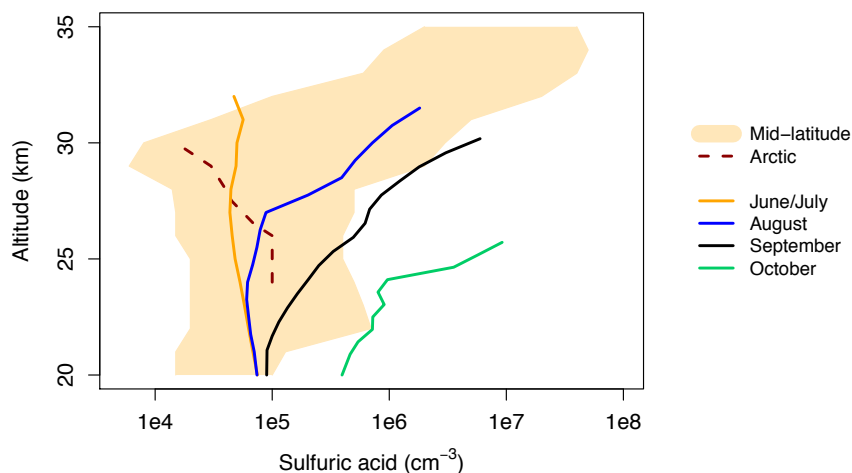
- Mills, M. J., Toon, O. B., Vaida, V., Hintze, P. E., Kjaergaard, H. G., Schofield, D. P., and Robinson, T. W. (2005). Photolysis of sulfuric acid vapor by visible light as a source of the polar stratospheric CN layer. *Journal of Geophysical Research: Atmospheres* (1984–2012), 110(D8).
- Reiner, T., and Arnold, F. (1997). Stratospheric SO₃: Upper limits inferred from ion composition measurements-
5 Implications for H₂SO₄ and aerosol formation. *Geophysical research letters*, 24(14), 1751-1754.
- Rosen, J. M., and Hofmann, D. J. (1983). Unusual behavior in the condensation nuclei concentration at 30 km. *Journal of Geophysical Research: Oceans* (1978–2012), 88(C6), 3725-3731.
- Schlager, H., and Arnold, F. (1987). Balloon-borne composition measurements of stratospheric negative ions and inferred sulfuric acid vapor abundances during the MAP/GLOBUS 1983 campaign. *Planetary and space science*, 35(5), 693-701.
- 10 Usoskin, I. G., Bazilevskaya, G. A., and Kovaltsov, G. A. (2011). Solar modulation parameter for cosmic rays since 1936 reconstructed from ground-based neutron monitors and ionization chambers. *Journal of Geophysical Research: Space Physics* (1978–2012), 116(A2).
- Vaida, V., Kjaergaard, H. G., Hintze, P. E., and Donaldson, D. J. (2003). Photolysis of sulfuric acid vapor by visible solar radiation. *Science*, 299(5612), 1566-1568.
- 15 Viggiano, A. A., and Arnold, F. (1981). Extended sulfuric acid vapor concentration measurements in the stratosphere. *Geophysical Research Letters*, 8(6), 583-586.
- Yu, F., and Turco, R. P. (1998). The formation and evolution of aerosols in stratospheric aircraft plumes: Numerical simulations and comparisons with observations. *Journal of Geophysical Research: Atmospheres* (1984–2012), 103(D20), 25915-25934.
- 20 Zhao, J., Toon, O. B., and Turco, R. P. (1995). Origin of condensation nuclei in the springtime polar stratosphere. *Journal of Geophysical Research: Atmospheres* (1984–2012), 100(D3), 5215-5227.



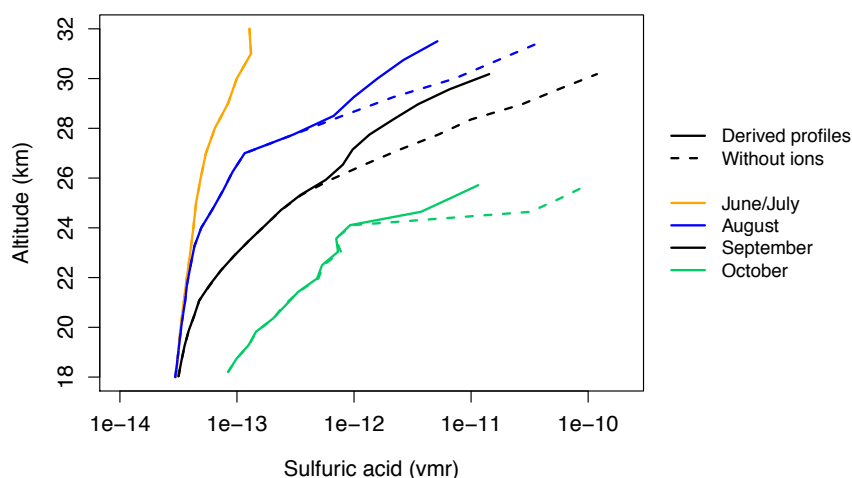
5 **Figure 1: Derivation of the “maximum trajectory” with model time steps of 1 month (a), and 5 days (b). Temperature (red), sulfuric acid (blue), and the other ambient conditions are changed at the beginning of each model time step (1 month or 5 days) and kept constant during the model time step while the CN (> 5 nm) concentrations (black) are simulated. The gaseous sulfuric acid was varied until the number concentration of CN particles matched the observations. At the beginning of each time step the CN concentration shifts abruptly as the changed ambient conditions lead to an adiabatic compression. The higher time resolution in b) breaks these big shifts into smaller more frequent shifts.**



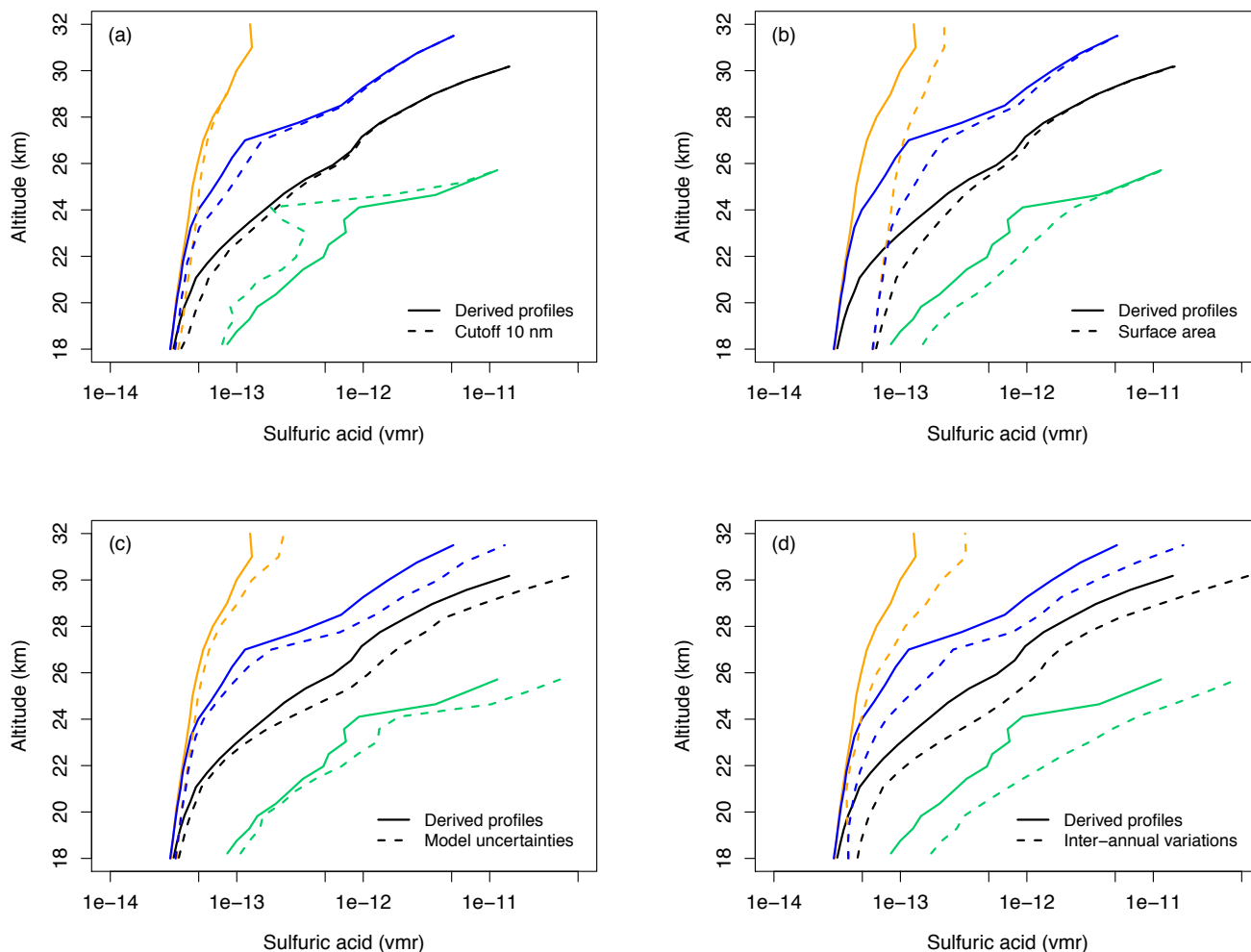
10 **Figure 2: The derived Antarctic sulfuric acid profiles corresponding to CN and temperature measurements above McMurdo, Antarctica (78°S) presented as concentration (a), and volume mixing ratio (b). The dotted line shows the unrealistic high October values (see discussion). The profiles are strongly correlated with temperature. Mixing ratios below 1e-12 also depend on preexisting particles surface area.**



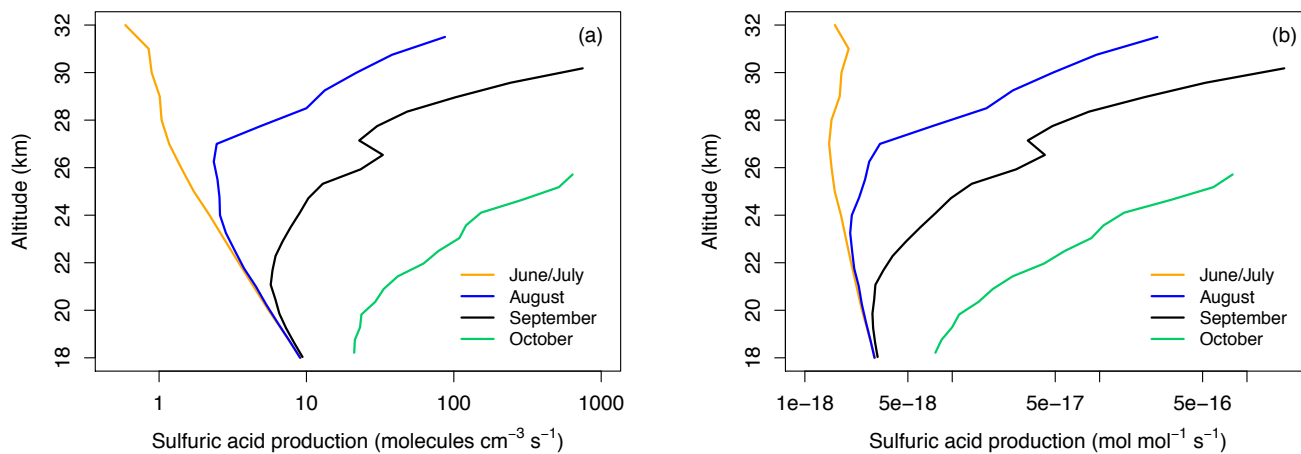
5 **Figure 3: Comparison of the derived Antarctic sulfuric acid profiles (solid lines) with mid latitude measurements and modeling of Arnold et al. (1981), Reiner and Arnold (1997), Schlager and Arnold (1987), Viggiano and Arnold (1981), and Mills et al. (2005) (shaded area) and inferred Arctic sulfuric acid from measurements presented by Krieger and Arnold (1994). The derived profiles have to be compared to mid-latitude concentrations at higher altitudes as the tropopause is lower over Antarctica.**



10 **Figure 4: Comparison of the sulfuric acid profiles derived including ion-induced nucleation (solid lines, reference profiles) and without simulating ions (dashed lines). In the area of lower temperatures (earlier and lower) the neutral clusters are stable enough so that the ions do not significantly change the nucleation rates. In the areas of higher temperatures (later and higher) the neutral clusters are not as stable anymore and more sulfuric acid is needed to reproduce the observed CN when ion-induced nucleation is not simulated.**



5 **Figure 5: Sensitivity studies varying (a) CN counter cutoff size, (b) preexisting particles surface area, (c) model parameters, and (d) inter-annual temperature and CN amounts, to estimate the uncertainties of the derived reference sulfuric acid profiles. The solid lines always show the derived reference profiles as presented in Fig. 2. The dashed lines show the profiles for model runs with the input values changed according to the sensitivity test. The October profile should have the highest uncertainty, followed by the June/July profile. The August and September profiles should be the most accurate. Detailed description of the varied parameters and discussion can be found in the text.**



5 **Figure 6: Estimates of sulfuric acid production rates presented per volume and second (a) and as mixing ratio per second (b). Some sulfuric acid production during the Antarctic winter is predicted. However, the modeling results should only be considered as first estimates as they are one additional step away from the measurements. Processes like preexisting particle evaporation, dark OH production (e.g. from cosmic rays), and CN production by other processes could change or could be included in these production profiles.**